

## Atom Interferometer Based on Bragg Scattering from Standing Light Waves

David M. Giltner, Roger W. McGowan, and Siu Au Lee

*Department of Physics, Colorado State University, Ft. Collins, Colorado 80523*

(Received 2 June 1995)

We have constructed an atom interferometer by Bragg deflecting a collimated beam of metastable neon atoms from three parallel standing waves. Interference fringes have been observed using atoms Bragg scattered at up to the third order, giving a maximum of  $6\hbar k$  transverse momentum difference between the two arms of the interferometer. In the first order case we have achieved a fringe contrast of 62% and a peak to peak signal of 1700 atoms/s. We believe this to be the highest fringe contrast that has been achieved in atom interferometers.

PACS numbers: 03.75.Dg, 07.60.Ly, 32.80.Lg

Atom interferometers are of interest due to their potential high sensitivity as inertial sensors for precision experiments in general relativity [1] and as spectrometers in probing atomic properties [2]. Potential applications also exist in nanometer-scale lithography. The atomic distribution in the interference pattern may be used either to directly deposit narrow lines [3] or to damage a resist material to make lithographic masks [4]. When extended to atoms with large nuclear spins or to large molecules, atom interferometry offers the possibility of studying macroscopic quantum coherence [5]. Even though several different atom interferometers have already been demonstrated [6–9], more work is needed in developing new designs which are more efficient, have better contrast, or are more accessible for implementation.

Atom interferometers use either microfabricated physical gratings or light beams to coherently split and recombine the atomic waves. The physical grating interferometers [6] can have large enclosed areas but spread the atom beam over many orders corresponding to different momentum states. This multiple beam scattering results in lowering the overall efficiency of the interferometer, and the multiple interfering beams are undesirable for some applications such as lithography. These disadvantages are shared by the recently demonstrated interferometer based on the Kapitza-Dirac scattering of atoms [7]. The optical Ramsey-Bordé interferometers using four traveling light waves [8] and light pulse interferometers [9] based on stimulated Raman transitions or adiabatic population transfer have, until now, achieved only small photon momentum difference between the interfering atoms [10]. In this paper we present the first demonstration of an atom interferometer based on Bragg scattering of atoms. Our interferometer is capable of coherently splitting a collimated neutral beam of atoms into only two beams at large angles and then recombining the atoms for interference. We have obtained atomic fringes corresponding to a six photon momenta difference between the two arms of the interferometer. This is the largest momentum difference that has been achieved in a matter-wave interferometer using light beams as optics.

The Bragg atom interferometer was first discussed by Dubetskii *et al.* in 1985 [11], and the Bragg scattering of atoms from a standing light wave was first observed with sodium in 1988 [12]. Our interferometer uses three near-resonant standing light waves to split and recombine the atoms. The two arms are of equal length, giving the interferometer a “white light” geometry. In our experiment we use metastable Ne atoms, but the choice of atoms is purely a matter of experimental convenience. We have investigated Bragg scattering extensively to characterize and improve the technique so that it is suitable for the optics in an atom interferometer. Details of our investigation will be reported elsewhere [13]. Up to sixth order Bragg scattering (with twelve photon momenta transfer) was obtained with good signal to noise and little contamination from other orders, and Fig. 1 shows typical Bragg deflection profiles, up to the third order, from a single standing wave.

Bragg scattering is an elastic multiphoton deflection process by which the atomic de Broglie waves are coherently diffracted by the periodic dipole potential in a near resonant standing wave (SW). The SW acts as a thick grating; therefore, the process is analogous to the diffraction of electrons by a crystal lattice. For atoms with de Broglie wavelength  $\lambda_{dB}$  scattered from a standing light wave of wavelength  $\lambda_L$ , the Bragg relation is given by

$$\lambda_L \sin\theta_n = n\lambda_{dB}, \quad (1)$$

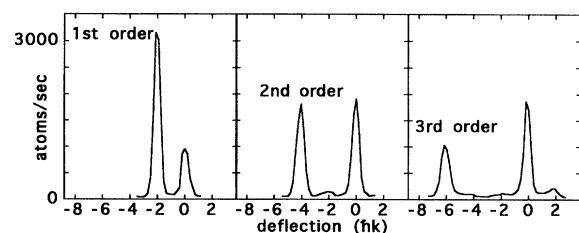


FIG. 1. Beam profiles for first through third order Bragg scattering of neon from a single standing wave. Undelected peaks are on the right. The SW radius was 6.0 mm, with a laser power of 30 mW.  $2\hbar k$  corresponds to  $\sim 58 \mu\text{rad}$  of deflection.

where  $\theta_n$  is the Bragg angle at which  $n$ th order scattering occurs. For effective Bragg scattering, the transverse dimension,  $2w_0$ , of the SW must be large so that the angular uncertainty in the photon momentum,  $\Delta\phi = \lambda_L/8\pi w_0$ , is substantially less than the angle between adjacent orders,  $2\theta_1$ . For scattering neon with  $\lambda_L = 640$  nm,  $2\theta_1 = 58$   $\mu$ rad and the SW radius  $w_0$  must be at least 3 mm. In addition, the incident atomic beam needs to be collimated to at least  $\theta_1$  to separate the two arms of the interferometer.

Bragg scattering has several attractive features for atom interferometry. First, it deflects atoms into only a single order, and the scattering order is under the control of the experimenter. The fraction of atoms deflected from each SW can be varied easily by adjusting either the SW intensity or the detuning of the light frequency from resonance. We are able to obtain deflection efficiencies from 0% to 80% for the neon atoms. In our interferometer, the intensities are adjusted such that the first and third SWs function as 50-50 beam splitters, and the second SW functions as two mirrors. Bragg scattering therefore provides a lossless, and potentially 100% efficient, atom optic. Second, a Bragg interferometer is easy to align, due to the fact that the atoms are deflected at discrete angles determined by the de Broglie and SW wavelengths. The laser intensity, detuning, and interaction time affect the deflection probability, but not the scattering angle. To align the interferometer, it is only necessary to adjust each SW independently for the desired scattering order. This ensures that the three SWs are parallel to each other, and atoms deflected by all three will automatically form the closed path that completes the interferometer. By choosing a higher Bragg order, the separation of the interferometer arms can be increased. Third, Bragg scattering involves only virtual transitions to the upper state, so that the atoms always remain in the lower state. Spontaneous emission, which destroys the coherence of the atomic beam, is not an issue during the free flight of the beams. This allows long arm lengths for the interferometer. In addition, since the atoms are in the same atomic state in the two paths of the interferometer, the atomic phase is not affected by temporal fluctuations in the SWs [14] and is less sensitive to external fields.

The experimental setup is shown in Fig. 2. Metastable neon was produced with a dc discharge in a supersonic nozzle source, and was collimated to  $<15$   $\mu$ rad by a 10  $\mu$ m slit and a 5  $\mu$ m slit separated by 90 cm. The average velocity of the atoms was about 1000 m/s  $\pm$  10%, but could vary, depending on the source condition. The nominal de Broglie wavelength was 19 pm. A dye laser was tuned near resonant with the  $1s_5(J=2)$ - $2p_0(J=3)$  transition in neon (640.2 nm). The linearly polarized laser beam was sent through a single mode fiber to provide a clean TEM<sub>00</sub> mode. It was then expanded to a radius of 4.5 mm, split into three beams separated by 31 cm, and retroreflected by three 1 in. diameter mirrors (flat

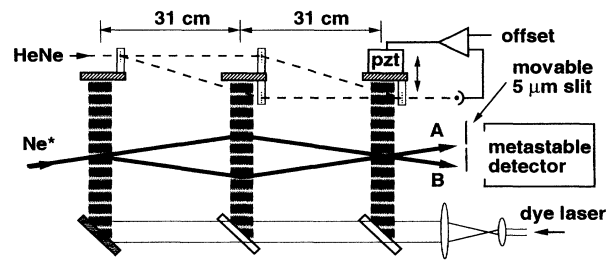


FIG. 2. Schematic of the Bragg interferometer. Metastable neon atoms are Bragg scattered by the three standing light waves to form interference fringes in beams A and B. Detector slit is used to select either beam. Dashed line shows path of helium-neon laser beam through gratings to form an auxiliary optical interferometer used for stabilization.

to  $\lambda/10$ ) to form the SWs. The flatness of the light beam wave fronts controls the quality of the atomic fringes, so it is important that the mirrors be of high quality. The horizontal and vertical angles of each mirror were adjusted to optimize scattering efficiency and fringe contrast. Fine adjustments in the horizontal angle were made with a piezoelectric transducer (PZT) mounted on the adjustment screw. The laser power in each SW was varied independently to produce the desired deflection probability, but typical values were 30 mW for the first and third SW (SW1 and SW3) and 65 mW for the second SW (SW2). The metastable atoms were detected with a Ceratron electron multiplier. The interferometer has two complementary output beams (A and B in Fig. 2). A movable 5  $\mu$ m slit was positioned in front of the detector to select one output beam. The detector was connected to an electrometer for beam current measurement, and to a preamplifier and discriminator for digital counting.

The interferometer was sensitive to vibration, and several measures were taken to ensure stability. The three mirrors used to create the SWs were mounted together into one assembly that could be aligned externally and then placed in the vacuum chamber. Rubber pads were used to reduce vibrations from the floor. Active stabilization was employed [6] to remove the remaining noise. Small gratings with 200 lines/mm were attached to the mirror mounts, as shown in Fig. 2, and a helium-neon laser beam was threaded through them to produce an auxiliary optical interferometer with the same geometry as the atomic one. The fringes produced by the optical interferometer were directed onto a photodiode whose signal displayed the relative position of the three mirrors. The third mirror was held in a special mount that allowed it to be translated by a PZT, and the final grating was attached directly to this mirror. The photodiode signal was fed back to the PZT to move the third mirror. Using this setup, we were able to hold the relative positions of the three mirrors to within 20 nm, or 6% of an atomic fringe.

To observe atomic interference, the detector slit was moved to either output A or B, and the position of the

third mirror was varied by changing the lock point of the feedback circuit. When the interferometer was scanned, fringes could be observed in real time in the beam current. Simultaneous measurements of the atom counts, registered by the metastable detector and the relative position of the third mirror detected by the photodiode, were made at a rate of 6 Hz, with each measurement lasting 17 ms. The recorded data were stored in a computer. Figure 3 shows the raw data of the count rate of detected atoms as the interferometer was scanned through 2.5 atomic periods. The high contrast atomic interference signal is clearly observable in real time.

Up to 4000 points were taken in a single run lasting about 11 min, and the data were binned and averaged according to the relative mirror position. The data were then fitted by a sine curve to determine the phase and contrast of the fringes. Typical processed data are shown in Fig. 4. Figure 4(a) shows the interference produced by atoms scattered at first order. The contrast is 62%, and the peak to peak fringe amplitude is 1700 atoms/s. We believe this to be the highest contrast that has been achieved from an atom interferometer. Figures 4(b) and 4(c) show the interference signals for second and third order scattering, with contrasts of 22% and 7%, respectively. The fringe period varies as  $1/n$ , as expected. The loss in contrast for higher orders is probably due to alignment errors between the three light beams. Additionally, we have not attempted to state select the atoms or to cancel stray electric and magnetic fields. The larger arm separation that results from higher order diffraction increases the susceptibility of the interferometer to field gradients.

Figure 5 shows the complementary interference signals measured for first order scattering from the two output beams. The two sets of data have equal contrasts (to within  $\pm 1\%$ ), indicating that SW1 was properly adjusted

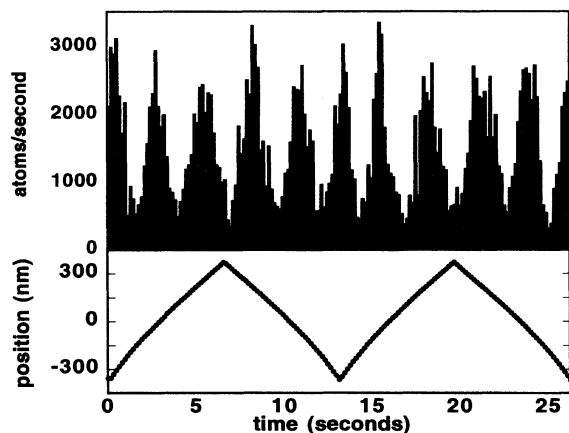


FIG. 3. Raw data as the interferometer is scanned over 2.5 fringes. Upper graph shows the number of atoms/s measured by the detector, and the lower graph shows mirror position. Atom fringes can be seen clearly in the upper graph.

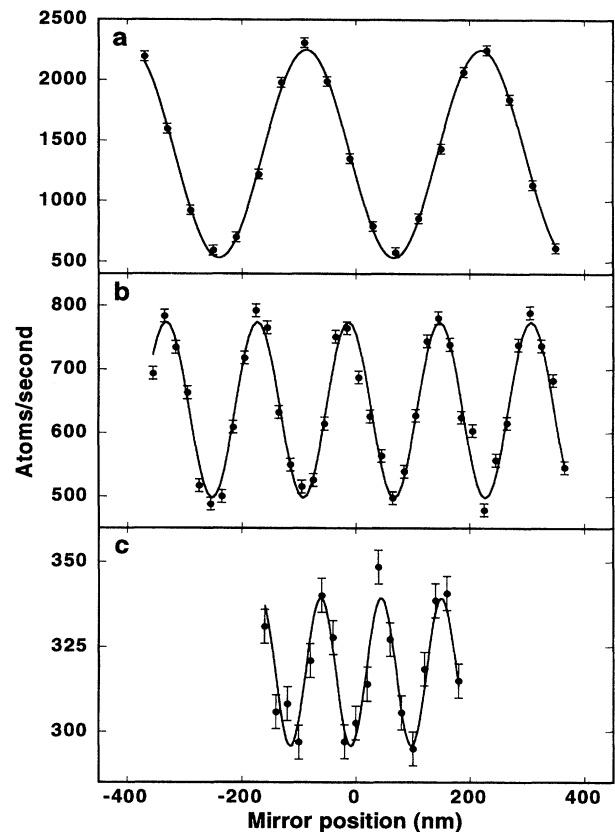


FIG. 4. Processed data showing atom fringes in Beam A of Bragg interferometer. Constant background of 50 atoms/s has been removed from each plot. The solid lines are fits to a sine curve. (a) First order deflection, 1000 points. Laser detuning  $\Delta = 2.5$  GHz. Laser power for SW1 and SW3 was 300 mW, and for SW2 was 65 mW. (b) Second order deflection, 4000 points,  $\Delta = 700$  MHz. Laser power for SW1 and SW3 was 30 mW, and for SW2 was 43 mW. (c) Third order deflection, 4000 points,  $\Delta = 500$  MHz. Laser power for SW1 and SW3 was 40 mW, and for SW2 was 58 mW.

as a 50-50 beam splitter. The difference in the fringe amplitudes and the slight phase shift from  $180^\circ$  between the two sets are due to the fact that it was difficult in our experiment to place the detector slit at exactly complementary positions.

In third order scattering, the two  $7 \mu\text{m}$  wide beams in our interferometer were separated by  $54 \mu\text{m}$ . This corresponds to a maximum enclosed area of  $17 \text{ mm}^2$ , which is almost 200 times the area of optical Ramsey-Bordé interferometers [2,8]. Larger areas are possible using higher order Bragg scattering and longer arm lengths. The transition probability for  $n$ th order Bragg deflection is given by [13]

$$P_n = \sin^2 \left[ \frac{\Omega_0^{2n} (w_0/V) \sqrt{\pi/2n}}{4^{2n-1} \Delta^n \epsilon^{n-1} [(n-1)!]^2} \right], \quad (2)$$

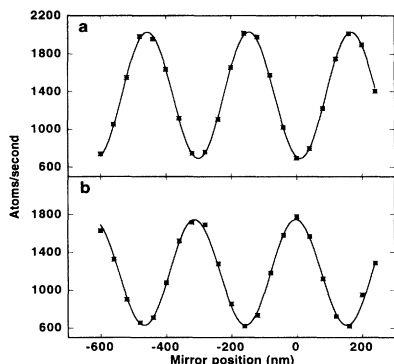


FIG. 5. Data showing complementary fringes exhibited by (a) beam A and (b) beam B. 4000 points were taken for each. The experimental conditions were not optimized, so that the fringe contrast was slightly lower than Fig. 4(a).

where  $\varepsilon = \hbar k^2/2M$  is the recoil frequency of the atom,  $w_0$  is the SW radius, and  $V$  is the atomic velocity. This result is valid for detuning  $\Delta$  much greater than the peak traveling wave Rabi frequency,  $\Omega_0$ , and the spontaneous linewidth,  $\Gamma$ . Equation (2) may be used to calculate the optimal laser intensity,  $I \propto \Omega_0^2$ , and detuning for higher order scattering. The probability for spontaneous emission varies as  $I/\Delta^2$ , and the condition for maintaining a constant Bragg scattering probability requires that  $I/\Delta$  be kept fixed. Therefore, by choosing the proper laser power and detuning, spontaneous emission can be reduced to the level where it is unimportant.

The Bragg interferometer can be used with a cold beam of atoms to drastically increase its area and improve its sensitivity. It is interesting to compare the capability of a cold atom interferometer as a gyroscope to that of a neutron interferometer. For a matter-wave interferometer of area  $A$  and using particles of mass  $m$ , the maximum fringe phase shift caused by an angular rotation frequency  $\Omega$  is  $\delta = 4\pi mA\Omega/h$ , where  $h$  is Planck's constant [1]. For example, we can reduce the velocity of the Ne atoms to 20 m/s using laser cooling techniques [15]. The 50-fold increase in area, coupled with the 20 times larger mass of the atoms, results in a gyroscopic sensitivity that will be at least 10 times over that of neutron interferometers. Another key advantage is that the atom

interferometer has higher flux and requires much less data acquisition time.

We would like to thank Christian Bordé for helpful discussions concerning atom interferometers. This work is supported by the National Science Foundation Consortium for Light Force Dynamics under Grant No. PHY-9312572.

- 
- [1] J. F. Clauser, *Physica (Amsterdam)* **151B**, 262 (1988).
  - [2] For an overview, see special issue on *Optics and Interferometry with Atoms* [Appl. Phys. B **54**, No. 5 (1992)]; see, also J. Schmiedmayer *et al.*, *Phys. Rev. Lett.* **74**, 1043 (1995).
  - [3] G. Timp *et al.*, *Phys. Rev. Lett.* **69**, 1636 (1992); J. J. McClelland *et al.*, *Science* **262**, 877 (1993).
  - [4] K. K. Berggren (private communication).
  - [5] A. Garg, *Phys. Rev. Lett.* **74**, 1458 (1995).
  - [6] D. W. Keith, C. R. Ekstrom, Q. A. Turchette, and D. E. Pritchard, *Phys. Rev. Lett.* **66**, 2693 (1991).
  - [7] E. Rasel *et al.*, preceding Letter, *Phys. Rev. Lett.* **75**, 2633 (1995).
  - [8] F. Riehle, Th. Kisters, A. Witte, J. Helmcke, and Ch. J. Bordé, *Phys. Rev. Lett.* **67**, 177 (1991); Ch. J. Bordé *et al.*, *Phys. Lett. A* **188**, 187 (1994); J. H. Müller *et al.*, *Appl. Phys. B* **60**, 199 (1995); K. Zeiske *et al.*, *Appl. Phys. B* **60**, 205 (1995).
  - [9] M. Kasevich and S. Chu, *Phys. Rev. Lett.* **67**, 181 (1991); M. Weitz, B. C. Young, and S. Chu, *Phys. Rev. Lett.* **73**, 2563 (1994).
  - [10] The Ramsey-Bordé interferometer is limited to a momentum difference of  $1\hbar k$  in the beams. In the light pulse interferometers of Ref. [6], although it is possible to transfer over  $140\hbar k$  of photon momentum between the two interferometer pairs, the interference fringe pattern is due only to a  $2\hbar k$  photon momentum difference between the two arms.
  - [11] B. Ya. Dubetskii, A. P. Kazantsev, V. P. Chebotaev, and V. P. Yakovlev, *Sov. Phys. JETP* **62**, 685 (1985).
  - [12] P. J. Martin, B. G. Oldaker, A. H. Miklich, and D. E. Pritchard, *Phys. Rev. Lett.* **60**, 515 (1988).
  - [13] D. M. Giltner, R. W. McGowan, and S. A. Lee, *Phys. Rev. A* (to be published).
  - [14] Ch. J. Bordé (private communication).
  - [15] A. Scholz, M. Christ, D. Doll, J. Ludwig, and W. Ertmer, *Opt. Commun.* **111**, 155 (1994).